Results in Physics 28 (2021) 104640

Contents lists available at ScienceDirect

Results in Physics

journal homepage: www.elsevier.com/locate/rinp

Improved optical and electrical properties for heterojunction solar cell using Al_2O_3/ITO double-layer anti-reflective coating

Muhammad Aleem Zahid [a,b], Muhammad Quddamah Khokhar [a], Ziyang Cui [a], Hyeonggi Park [a,*], Junsin Yi [a,*]

[a] Department of Electrical and Computer Engineering, Sungkyunkwan University, Suwon, Gyeonggi-Do 16419, South Korea
[b] Electrical Engineering Department, University of Engineering & Technology, Taxila 47050, Pakistan

ARTICLE INFO

Keywords:
Silicon heterojunction solar cell
Double layered anti-reflection coating
Optical Properties
Electrical Properties

ABSTRACT

Silicon heterojunction solar cells have been gaining remarkable attention in the photovoltaic industry in recent years owing to their low temperature coefficient and high efficiency. This study aimed to maximize the short circuit current density (J_{sc}), which is directly correlated with the absorbance of the solar cells. An advanced ray tracking model and hall effect measurement was used to improve the optical properties of Al_2O_3/ITO as a double-layered anti-reflection coating (DLARC) on the solar cell. RF/DC power sputtering system was used to deposit ITO layer, while atomic layer deposition was used to deposit Al_2O_3 on ITO to create a DLARC. An average decrease in reflection from 9.33% to 4.74% and enhancement in EQE from 76.89% to 84.34% were observed for the DLARC in the wavelength spectrum at 300–1100 nm. It also exhibited a higher J_{sc} value of 41.13 mA/cm^2 and maximum conversion efficiency of 21.6%. The findings of both simulation and experiments showed that the Al_2O_3/ITO DLARC has better anti-reflection properties than a single-layer ITO coating.

Introduction

Silicon heterojunction (SHJ) solar cell is getting considerable interest in photovoltaic research and have been extensively studied. High efficiency SHJ solar cells are produced by linking the amorphous silicon (a-Si) and crystalline silicon (c-Si) technologies [1–6]. They have a cost-effective fabrication process along with an improved temperature coefficient when compared with standard c-Si solar cell [3–9]. Furthermore, SHJ solar cells are suitably shaped for applications in thin c-Si wafer. [10]. However, cells made with a thin wafer has low absorption efficiency in the red and near-infrared portions of the solar spectrum resulting in a lower J_{sc}. The hydrogenated a-Si (a-Si:H) emitter layer causes excessive reflection losses in SHJ solar cells owing to their high refractive index [11]. Therefore, lowering the optical losses would improve the absorption properties of a solar cell, which is the crucial aspect for attaining high efficiency. Accordingly, these cells must have excellent anti-reflection activity to trap light. Current SHJ solar cells utilize pyramidal texturing through alkali etching to achieve proper light trapping and anti-reflection properties [12–14]. Transparent conductive oxide (TCO) on a textured surface reduces reflectance while also increasing the injection of photons from the solar spectrum into the device [12,13,15–18]. TCO layer optimization in SHJ solar cell needs to balance series resistance, optical and recombination losses [19]. The TCO criteria include, but are not restricted to the following: (1) the refractive index should be less than 2 to assist as an anti-reflection coating (ARC) on a silicon wafer; (2) the front contact layer should be transparent in the wavelength spectrum of 300–1100 nm; (3)TCO on the front side of the cell should have the required lateral conductivity [19]; (4) both TCOs should be able to make strong ohmic interactions with doped a-Si films and corresponding metal electrodes where there is a possibility to form Schottky barriers [20]; and (5) the underlying a-Si layer should not be damaged by TCO deposition [21] and it should not cause any interaction that would lower the SHJ solar cell's efficiency in the c-Si/a-Si heterojunction [22]. The TCO material indium tin oxide (ITO) fulfills the aforementioned requirements and is widely used in SHJ solar cell technology [23–26]. ITO is also used for an antireflection purpose in SHJ solar cell [11]. Multilayer ARC is observed to be the most effective structure for optimizing the performance of SHJ solar cells

Abbreviations: SHJ, Silicon heterojunction; a-Si, Amorphous silicon; c-Si, Crystalline silicon; a-Si:H, hydrogenated a-Si; ARC, Anti-reflection coating; SLARC, Single layer anti reflection coating; DLARC, Double layer anti reflection coating; TCO, Transparent conductive oxide; ITO, Indium Tin Oxide; Al_2O_3, Aluminium Oxide; AM, Air Mass; EQE, External quantum efficiency.

* Corresponding authors.

https://doi.org/10.1016/j.rinp.2021.104640
Received 25 May 2021; Received in revised form 20 July 2021; Accepted 31 July 2021
Available online 5 August 2021

through the minimization of incident solar radiation reflectance losses [27–30]. Moreover, adding a dielectric coating on the top of the TCO layer lowers the cost and enhances the stability and efficiency of the solar cell and module [31]. The dielectric Al_2O_3 coating have gained popularity owing to their excellent stability, high dielectric strength, toughness under harsh conditions and high transparency [32]. In recent years, Al_2O_3 coatings have been used in a variety of practical applications such as refractory coatings, anti-corrosive coatings [33], and anti-reflective coatings [27,34]. The addition of Al_2O_3 on TCO layer is promising for enhancing the efficiency of SHJ solar cell. To best of our knowledge, the antireflection effect of dielectric layer Al_2O_3 on the top of ITO has not been practically analyzed for SHJ solar cell and it need to be thoroughly investigated.

This work is supported by simulation, designing, and fabrication of a Al_2O_3/ITO DLARC on textured SHJ solar cells and investigation of its optoelectronic properties in the wideband spectrum of 300 to 1100 nm. The focus is to maximize the light absorbance in the cell, thereby enhancing J_{sc}. The optimized thickness of DLARC was adjusted by having a tradeoff between optical and electrical properties. The desired solar cell was then fabricated to validate the simulation design for maximizing the efficiency.

Experimental

The p-doped czochralski-grown monocrystalline Si wafer (160 μm,1–10 Ω) was utilized for the fabrication of the desired SHJ solar cell. The typical RCA-1 and RCA-2 process supported by ultrasonic treatment was used to clean the Si wafer. Plasma-enhanced chemical vapor deposition was used under a SiH_4:H_2: B_2H_6 (1%) environment with a gas ratio of 3:22:0.09, power of 14mW cm^2, chamber temperature of 200 °C and a deposition pressure of 100 mTorr. Using this system, a-Si:H(i) films having a thickness of 5 nm were deposited on both sides of the wafer. Consequently, 7 nm a-Si:H(n) and a-Si:H(p) films were added to the front and rear of the wafer, respectively. RF/DC sputtering system having 300/200 W power with a target which was made up of 90 wt% In_2O_3 and 10 wt% SnO_2 with 99.999% purity (purchased from baco solution) was used to deposit ITO layer on the glass (eagle 2000, Corning) and silicon wafer having a thickness of 70 nm. While, on the rear part of the cell, the thick 130 nm ITO film was deposited. Argon gas (30 sccm) was utilized for the sputtering process at a chamber temperature of 180 °C. ITO deposition was completed by placing a metallic mask on the a-Si layer to make a shaped ITO. A high vacuum with an initial pressure of 10^{-5} Torr and a working pressure of 10^{-3} Torr was created. Silver paste was used to fabricate metallic electrodes using a low-temperature screen printing process. Finally, NCD Lucida D100 atomic layer deposition system was used to deposit 50 nm Al_2O_3 on ITO to create a DLARC. A schematic illustration of the textured SHJ solar cell with Al_2O_3/ITO as a DLARC is depicted in Fig. 1.

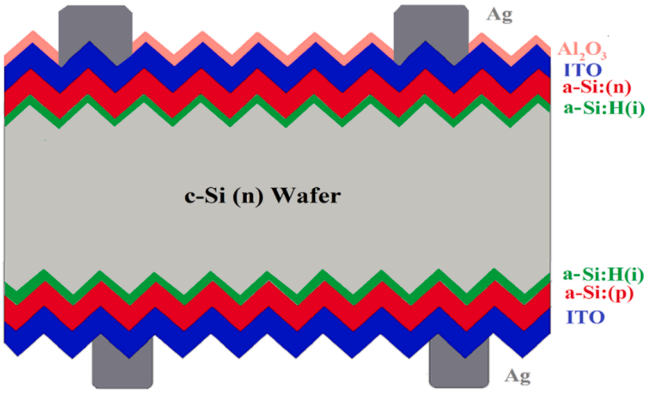

Fig 1. Fabricated structure of SHJ solar cell having an Al_2O_3/ITO DLARC.

The thickness and refractive index measurement of ITO and Al_2O_3 layers was done by using spectroscopic ellipsometry system (Nano view, MF-1000) and spectroscopic ellipsometer (Elli-SE-1000). The sheet resistance of ITO layer was calculated using a hall effect measurement system (Ecopia HMS-3000). The reflectance and transmittance were measured by an ultra-violet spectrophotometer (SCINCO-3100). The surface morphology of the DLARC films was seen through field emission scanning electron microscopy (JEOL JSM-7600F). The external quantum efficiency (EQE) of the textured SHJ solar cell was investigated using a spectral response measurement system (QE/IPCE, QEX7). The electrical parameters of the fabricated SHJ solar cell were analyzed using current density–voltage (*J-V*) technique in Air Mass (*AM*) 1.5, 1 sun illumination conditions (100 mW/cm^2). OPAL-2 software by PV Lighthouse was used to perform an optical simulation to optimize the thickness and optical properties of the Al_2O_3/ITO DLARC [35].

Results and Discussions

To evaluate the suitability of ARC on a fabricated cell, it is necessary to consider the *AM* 1.5 solar spectrum [36] as shown in Fig. 2. The wavelength spectrum between 300 and 1100 nm was selected for the research, because the spectral power density for wavelengths shorter than 300 nm is negligible, while the upper wavelength for useful irradiation for c-Si is 1100 nm [37].

Optical simulation for SHJ solar cell

The textured SHJ solar cell was used to perform the optical simulation. It is established that the average weighted reflectance ($\overline{R}$) of the textured surface is considerably lower than that of flat smooth polished surface due to light gets opportunity to strike multiple points on the textured surface and more possible ways to enter the wafer as shown in Fig. 3(a) [11]. A ray-tracing model was utilized to simulate the DLARC on a textured pyramid surface. The pyramids were randomly distributed with an angle of 54.7°. As the bandgap energy of c-Si is 1.1 eV [30], so the absorbable wavelength region up to 1100 nm was considered. First, the weighted average absorbance ($\overline{A}_{c\text{-}Si}$) in c-Si with ITO single-layer anti-reflective coating (SLARC) was computed relative to the ITO thickness, as depicted in Fig. 3(b) [11]. The figure shows that the maximum $\overline{A}_{c\text{-}Si}$ can be obtained when the thickness of ITO is ~ 70 nm. The same ITO thickness was previously calculated for textured SHJ solar cells [11].

The refractive index values of ITO and Al_2O_3 at 550 nm are ~ 1.9

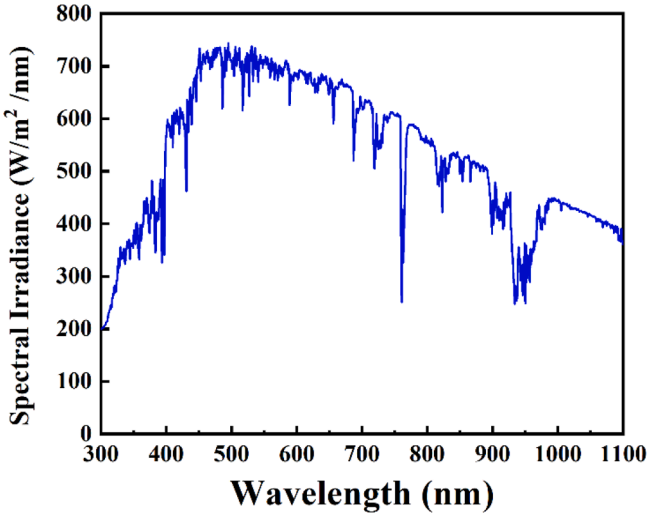

Fig 2. Photon flux density as a function of wavelength for solar spectrum of *AM* 1.5.

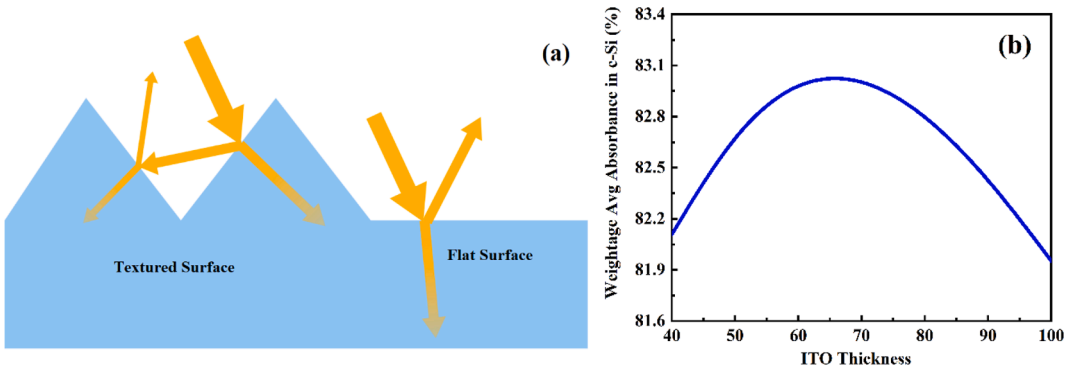

Fig 3. (a) Representation of light path in flat and textured surface. (b) $\overline{A}_{c\text{-}Si}$ by varying the ITO thickness.

and ~ 1.7, respectively. Given that the refractive index of Al_2O_3 is located between that of air and ITO, it may be added on the ITO surface to create a DLARC. $\overline{A}_{c\text{-}Si}$ and $\overline{R}$ at varying ITO/Al_2O_3 coating thicknesses was analyzed using simulation tool, as shown in Fig. 4(a, b). It was observed that 60 nm ITO shows minimum $\overline{R}$ and maximum $\overline{A}_{c\text{-}Si}$ but the sheet resistance (R_{sheet}) at this thickness was higher than those of higher ITO thicknesses. Fig. 4 (c) shows the R_{sheet} values at varying ITO thicknesses. Increasing the ITO thickness increases the parasitic light absorption from the TCO itself [31]. This parasitic absorption would a hinderance in the absorption of light in c-Si and limiting the conversion efficiency [38]. A trade-off between optical and electrical properties was used to achieve optimum efficiency performance. The R_{sheet} of 70 nm ITO (70 Ω/sq) is less than that of 60 nm ITO (86 Ω/sq). Moreover, the $\overline{R}$ and $\overline{A}_{c\text{-}Si}$ for 50/70 nm Al_2O_3/ITO are better than those of other DLARC Al_2O_3/ITO thicknesses. Therefore, 50/70 nm Al_2O_3/ITO as the DLARC thickness was chosen to maximize the efficiency of the textured SHJ solar cell.

Surface Morphology

To reduce the surface reflection and increase the light absorbance, a Al_2O_3/ITO DLARC with a thickness of 50/70 nm was deposited. The corresponding scanning electron microscopy image showing the surface morphology with a cross-sectional view is shown in Fig. 5. The 3D morphological textured surface of the SHJ solar cell, where pyramids can be easily observed, is shown in Fig. 5(a). The cross-sectional view of Al_2O_3/ITO layers deposited on the solar cell (Fig. 5(b)) indicates no intermediate layer is present.

Optical Properties

The DLARC can significantly minimize the optical loss in the cell. To

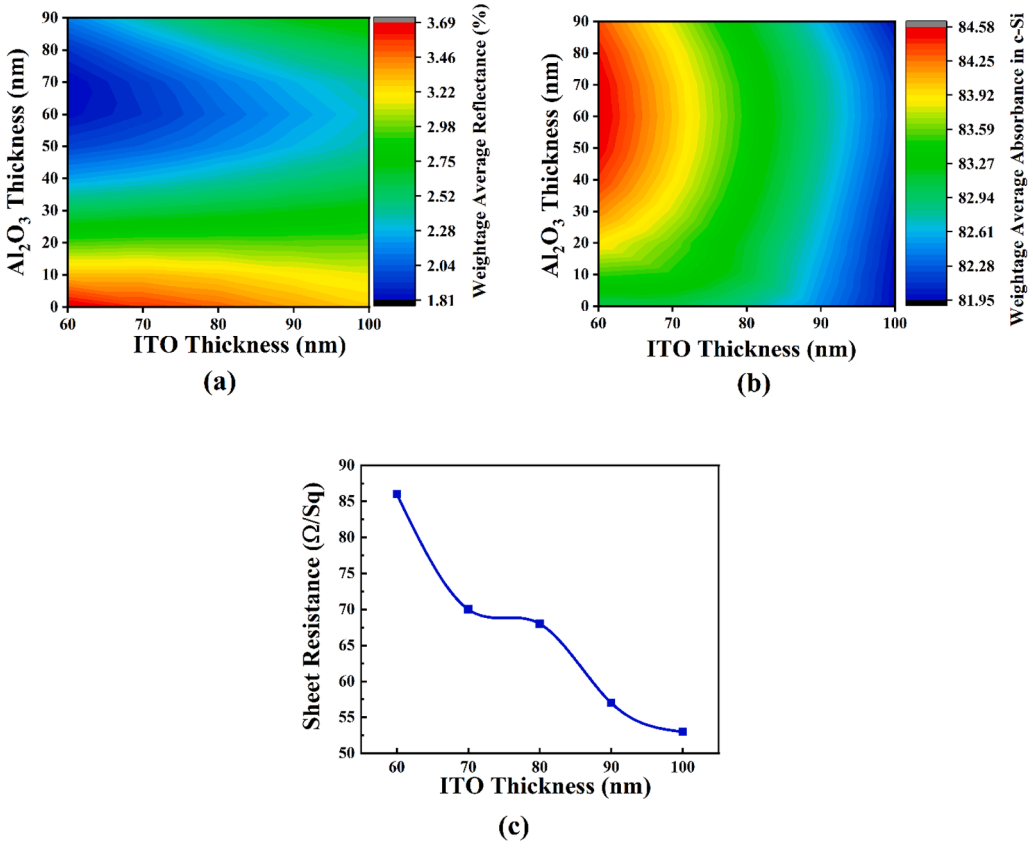

Fig 4. The simulated (a) $\overline{R}$ and (b) $\overline{A}_{c\text{-}Si}$ in relation to the ITO and Al_2O_3 thickness. (c) Variation of sheet resistance of ITO with thickness.

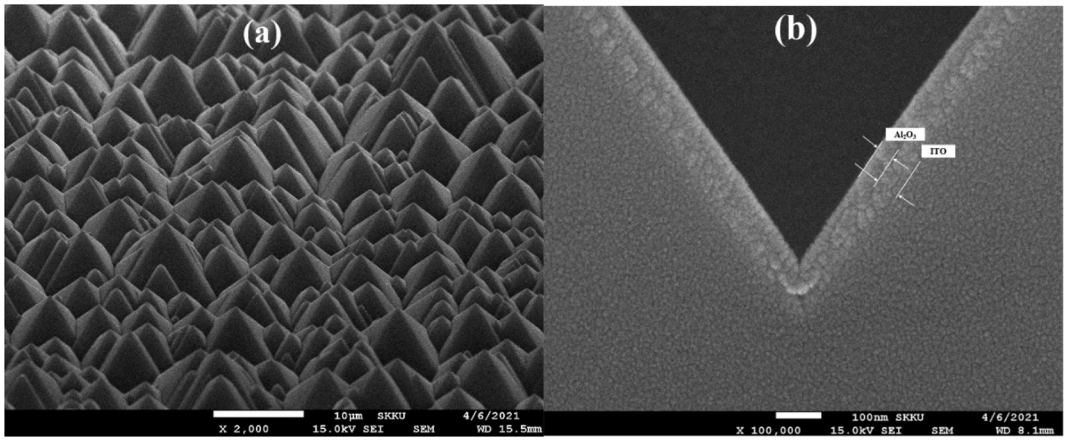

Fig 5. (a) The 3D morphological view and (b) cross-sectional view of the Al_2O_3/ITO layers on top of the cell.

quantitatively analyze the optical properties of DLARC, the study of refractive index of a material was carried out. The DLARC was considered as an optical material having different refractive index stack together. The average refractive index of Al_2O_3 and ITO for the wavelength spectrum of 300–1100 nm are 1.71 and 1.95, respectively. The refractive index values in DLARC increases from top to bottom layer. It reduced the energy loss and enhanced the performance of DLARC. Fig. 6 shows the refractive indexes of Al_2O_3 and ITO material for the wavelength region of 300–1100 nm.

The average transmittance and reflectance of the 70 nm ITO layer were 84.29% and 7.87% respectively for wavelength spectrum of 300–1100 nm. For Al_2O_3/ITO DLARC, it was 86.95% and 6.63%, respectively. The reflectance and transmittance of the ITO SLARC coating and Al_2O_3/ITO DLARC were computed after experiment and are shown in Fig. 7.

An increase in transmission by 3.05% and a decrease in reflectance by 15.76% can be observed for having DLARC. In the wavelength spectrum of 400–700 nm, the average transmittance and reflectance of the SLAR ITO layer were 81.97% and 9.39%, respectively. Meanwhile, it was 92.05% and 4.33%, respectively for the DLARC, possessing an increase in transmission of 10.95% and a decrease in reflectance of 53.89%. Moreover, the reflectance measurement on SHJ solar cell showed that $\overline{R}$ reduced from 9.33% in case of ITO SLARC to 4.74% in the case of Al_2O_3/ITO DLARC for the wavelength spectrum of 300–1100 nm.

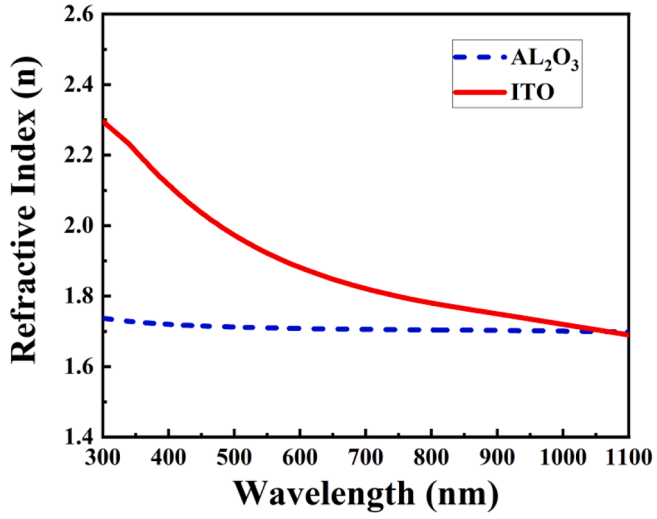

Fig 6. Measured refractive indices of ITO and Al_2O_3 in the wavelength spectrum of 300–1100 nm.

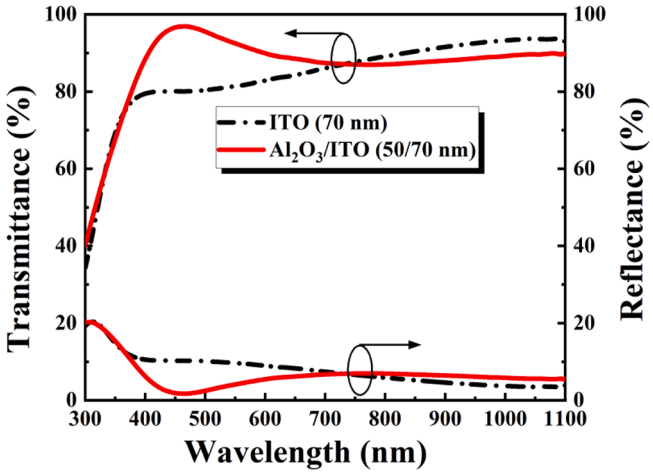

Fig 7. Optical reflectance and transmittance of Al_2O_3/ITO DLARC on a glass substrate.

The reduction in $\overline{R}$ from 7.37% in case of ITO SLARC to 1.69% in the case of Al_2O_3/ITO DLARC for the wavelength spectrum of 500–1000 nm as shown in Fig. 9. This reduction in reflection causes more light to be trapped on the solar cell. Furthermore, the improved optical properties indicate more photocurrent in the solar cell, and hence the conversion efficiency of the fabricated SHJ solar cell was enhanced favorably.

Electrical Properties

After meaningful enhancement in the optical properties, similar improvements in the electrical properties are expected for Al_2O_3/ITO DLARC. The J_{sc} of a PV device is an important parameter to describe its power conversion efficiency [39–41]. A J_{sc} map at the AM 1.5G spectrum is very valuable because it predicts the final J_{sc} output after catering all the optical and electrical losses in a complete solar cell [41]. The J_{sc} and efficiency (η) of the ITO SLARC were 39.91 mA/cm^2 and 20.95%, respectively. The Al_2O_3/ITO DLARC exhibited a higher J_{sc} and η of 41.13 mA/cm^2 and 21.60% respectively which is 2.97% and 3% higher than those of the ITO SLARC. Fig. 8 shows the *J-V* curves of the ITO SLARC and Al_2O_3/ITO DLARC.

The EQE calculates the total number of electrons leaving the cell divided by the total sum of incident photons at every wavelength [42]. EQE analysis is extremely important for examining the influence of the ARC on the complete performance of SHJ solar cells [43]. The average EQE enhancement from 76.89% to 84.34% was observed in the

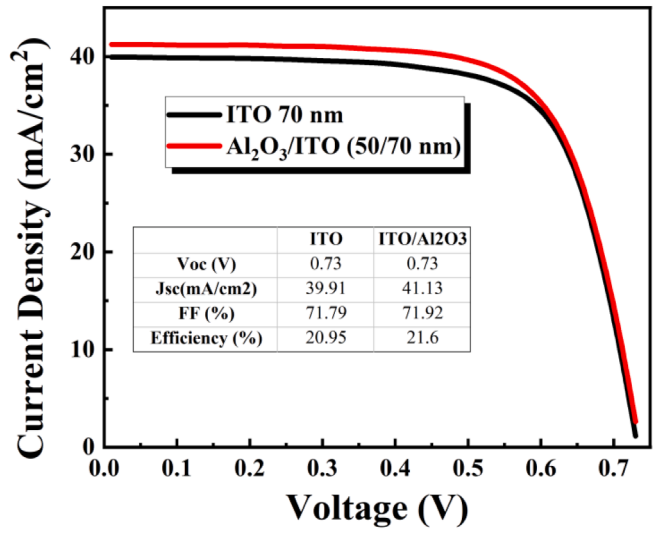

Fig 8. *J-V* curves of textured SHJ solar cell having ITO SLARC and Al_2O_3/ITO DLARC.

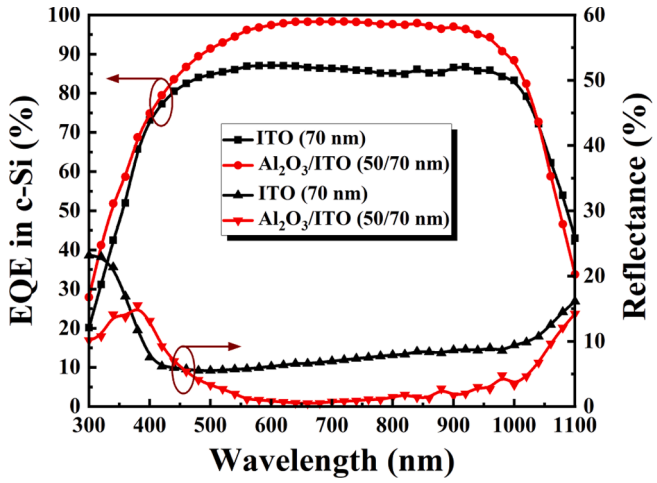

Fig 9. EQE and Reflectance measurement of textured SHJ solar cell having SLAR ITO and DLAR Al_2O_3/ITO coating.

wavelength spectrum of 300–1100 nm. The addition of Al_2O_3 layer shows significant increase in the EQE for mostly visible and near infrared wavelength region. The increase in EQE from 85.87% to 96.20% was observed in the wavelength spectrum of 500–1000 nm as shown in Fig. 9. The EQE curve shows that Al_2O_3 layer can effectively improve the J_{sc} of the solar cell. The J_{sc} increased from 39.91 mA/cm^2 to 41.13 mA/cm^2 because of EQE enhancement which is directly related to absorbance in the solar cell. This EQE enhancement for Al_2O_3/ITO DLARC effectively increases the J_{sc} of 1.22 mA/cm^2 when compared with ITO SLARC. The EQE and reflectance curves for the ITO SLARC and optimized Al_2O_3/ITO DLARC are shown in Fig. 9.

The graph shows higher EQE values for the entire wavelength range, except for wavelength over >~1040 nm. This is assumed that the light with a higher wavelength reflects less in SLARC than DLARC; however, it would not significantly affect the performance of the cell. Therefore, the overall DLAR exhibited improved electrical properties.

Conclusion

This work is focused on the fabrication and investigation of an SHJ solar cell with Al_2O_3/ITO as a DLARC on the front side based on the maximum average absorbance. Both the simulated and experimental results shows that the Al_2O_3/ITO DLARC has better anti-reflection effect which improves the optical and electrical properties. The fabricated textured SHJ solar cell with the Al_2O_3/ITO DLARC exhibited enhancement in EQE from 76.89% to 84.34%, reduction of average reflectance from 9.33% to 4.74% and an increase in J_{sc} from 39.91 mA/cm^2 to 41.13 mA/cm^2 as compared to the ITO SLARC. The improved optical and electrical properties lead to increase the cell efficiency from 20.95% to 21.60%. These results suggest that the fabricated Al_2O_3/ITO DLARC can be effectively used in industrial SHJ solar cell applications.

CRediT authorship contribution statement

Muhammad Aleem Zahid: Conceptualization, Data curation, Formal analysis, Investigation, Methodology, Software, Validation, Writing - original draft, Writing - review & editing. **Muhammad Quddamah:** Data curation, Resources. **Ziyang Cui:** Data curation, Resources. **Hyeonggi Park:** Investigation, Project administration, Visualization, Writing - review & editing, Funding acquisition. **Junsin Yi:** Funding acquisition, Supervision.

Declaration of Competing Interest

The authors declare that they have no known competing financial interests or personal relationships that could have appeared to influence the work reported in this paper.

Acknowledgment

This research was supported by Korea Initiative for fostering University of Research and Innovation Program of the National Research Foundation (NRF) funded by the Korean government (MSIT) (No.2020M3H1A1077095).

References

[1] Hussain SQ, Kim S, Ahn S, Balaji N, Lee Y, Lee JH, et al. Influence of high work function ITO: Zr films for the barrier height modification in a-Si: H/c-Si heterojunction solar cells. Sol Energy Mater Sol Cells 2014;122:130–5.
[2] Hussain SQ, Kim S, Ahn S, Park H, Le AHT, Lee S, et al. RF magnetron sputtered ITO: Zr thin films for the high efficiency a-Si: H/c-Si heterojunction solar cells. Met Mater Int 2014;20(3):565–9.
[3] Mishima T, Taguchi M, Sakata H, Maruyama E. Development status of high-efficiency HIT solar cells. Sol Energy Mater Sol Cells 2011;95(1):18–21.
[4] Taguchi M, Yano A, Tohoda S, Matsuyama K, Nakamura Y, Nishiwaki T, et al. 24.7% record efficiency HIT solar cell on thin silicon wafer. IEEE J Photovoltaics 2014;4(1):96–9.
[5] Tanaka M, Okamoto S, Tsuge S, Kiyama S. Development of HIT solar cells with more than 21% conversion efficiency and commercialization of highest performance HIT modules. 3rd World Conference onPhotovoltaic Energy Conversion, 2003. Proceedings of, vol. 1, IEEE; 2003, p. 955–8.
[6] Tsunomura Y, Yoshimine Y, Taguchi M, Baba T, Kinoshita T, Kanno H, et al. Twenty-two percent efficiency HIT solar cell. Sol Energy Mater Sol Cells 2009;93(6-7):670–3.
[7] Park H, Lee Y-J, Park J, Kim Y, Yi J, Lee Y, et al. Front and back TCO research review of a-Si/c-Si heterojunction with intrinsic thin layer (HIT) solar cell. Trans Electr Electron Mater 2018;19(3):165–72.
[8] Dao VA, Choi H, Heo J, Park H, Yoon K, Lee Y, et al. rf-Magnetron sputtered ITO thin films for improved heterojunction solar cell applications. Curr Appl Phys 2010;10(3):S506–9.
[9] Wada H, Nishikubo K, Sichanugrist P, Konagai M. Improved light trapping effect for thin-film silicon solar cells fabricated on double-textured white glass substrate. Can J Phys 2014;92(7/8):920–3.
[10] Tohoda S, Fujishima D, Yano A, Ogane A, Matsuyama K, Nakamura Y, et al. Future directions for higher-efficiency HIT solar cells using a thin silicon wafer. J Non-Cryst Solids 2012;358(17):2219–22.
[11] Zhang D, Digdaya IA, Santbergen R, van Swaaij RACMM, Bronsveld P, Zeman M, et al. Design and fabrication of a SiOx/ITO double-layer anti-reflective coating for heterojunction silicon solar cells. Sol Energy Mater Sol Cells 2013;117:132–8.
[12] Olibet S, Monachon C, Hessler-Wyser A, Vallat-Sauvain E, Fesquet L, Damon-Lacoste J, et al. Textured silicon heterojunction solar cells with over 700mV open-circuit voltage studied by transmission electron microscopy. 2008.
[13] Li G, Zhou Y, Liu F. Influence of textured c-Si surface morphology on the interfacial properties of heterojunction silicon solar cells. J Non-Cryst Solids 2012;358(17):2223–6.

[14] Kang MG, Tark S, Lee JC, Son C-S, Kim D. Changes in efficiency of a solar cell according to various surface-etching shapes of silicon substrate. J Cryst Growth 2011;326(1):14–8.
[15] Wang Qi, Xu Y, Iwaniczko E, Page M. Light trapping for high efficiency heterojunction crystalline Si solar cells. ECS Trans 2011;34(1):1129–34.
[16] Fesquet L, Olibet S, Damon-Lacoste J, De Wolf S, Hessler-Wyser A, Monachon C, et al. Modification of textured silicon wafer surface morphology for fabrication of heterojunction solar cell with open circuit voltage over 700 mV. 2009 34th IEEE Photovoltaic Specialists Conference (PVSC), IEEE; 2009, p. 754–8.
[17] Lien S-Y, Yang C-H, Hsu C-H, Lin Y-S, Wang C-C, Wuu D-S. Optimization of textured structure on crystalline silicon wafer for heterojunction solar cell. Mater Chem Phys 2012;133(1):63–8.
[18] Jeong D, Kim C, Song J, Lee JC, Cho JS, Park SH, et al. Effect of texture morphology on the surface passivation and a-Si/c-Si heterojunction solar cells. 2009 34th IEEE Photovoltaic Specialists Conference (PVSC), IEEE; 2009, p. 642–5.
[19] Herasimenka SY, Dauksher WJ, Boccard M, Bowden S. ITO/SiOx: H stacks for silicon heterojunction solar cells. Sol Energy Mater Sol Cells 2016;158:98–101.
[20] Bivour M, Schröer S, Hermle M. Numerical analysis of electrical TCO/a-Si: H (p) contact properties for silicon heterojunction solar cells. Energy Procedia 2013;38:658–69.
[21] Demaurex B, De Wolf S, Descoeudres A, Charles Holman Z, Ballif C. Damage at hydrogenated amorphous/crystalline silicon interfaces by indium tin oxide overlayer sputtering. Appl Phys Lett 2012;101(17):171604. https://doi.org/10.1063/1.4764529.
[22] Tomasi A, Sahli F, Seif JP, Fanni L, de Nicolas Agut SM, Geissbuhler J, et al. Transparent electrodes in silicon heterojunction solar cells: influence on contact passivation. IEEE J Photovoltaics 2016;6(1):17–27.
[23] Balestrieri M, Pysch D, Becker J-P, Hermle M, Warta W, Glunz SW. Characterization and optimization of indium tin oxide films for heterojunction solar cells. Sol Energy Mater Sol Cells 2011;95(8):2390–9.
[24] Ritzau K-U, Behrendt T, Palaferri D, Bivour M, Hermle M. Hydrogen doping of indium tin oxide due to thermal treatment of hetero-junction solar cells. Thin Solid Films 2016;599:161–5.
[25] Aïssa B, Abdallah AA, Zakaria Y, Kivambe MM, Samara A, Shetty AR, et al. Impact of the oxygen content on the optoelectronic properties of the indium-tin-oxide based transparent electrodes for silicon heterojunction solar cells. AIP Conference Proceedings, vol. 2147, AIP Publishing LLC; 2019, p. 30001.
[26] Haschke J, Lemerle R, Aissa B, Abdallah AA, Kivambe MM, Boccard M, et al. Annealing of silicon heterojunction solar cells: interplay of solar cell and indium tin oxide properties. IEEE J Photovoltaics 2019;9(5):1202–7.
[27] Zhao L, Zhou CL, Li HL, Diao HW, Wang WJ. Role of the work function of transparent conductive oxide on the performance of amorphous/crystalline silicon heterojunction solar cells studied by computer simulation. Physica Status Solidi (A) 2008;205(5):1215–21.
[28] Jensen N, Hausner RM, Bergmann RB, Werner JH, Rau U. Optimization and characterization of amorphous/crystalline silicon heterojunction solar cells. Prog Photovoltaics Res Appl 2002;10(1):1–13.
[29] Bahrami A, Mohammadnejad S, Abkenar NJ, Soleimaninezhad S. Optimized single and double layer antireflection coatings for GaAs solar cells. Int J Renew Energy Res (IJRER) 2013;3:79–83.
[30] Kim S, Jung J, Lee Y-J, Ahn S, Hussain SQ, Park J, et al. Role of double ITO/In2O3 layer for high efficiency amorphous/crystalline silicon heterojunction solar cells. Mater Res Bull 2014;58:83–7.
[31] Du G, Bai Y, Huang J, Zhang J, Wang J, Lin Y, et al. Surface passivation of ITO on heterojunction solar cells with enhanced cell performance and module reliability. ECS J Solid State Sci Technol 2021;10(3):035008. https://doi.org/10.1149/2162-8777/abeece.
[32] Shamala KS, Murthy LCS, Narasimha Rao K. Studies on optical and dielectric properties of Al2O3 thin films prepared by electron beam evaporation and spray pyrolysis method. Mater Sci Eng, B 2004;106(3):269–74.
[33] Yan D, He J, Li X, Liu Y, Zhang J, Ding H. An investigation of the corrosion behavior of Al2O3-based ceramic composite coatings in dilute HCl solution. Surf Coat Technol 2001;141(1):1–6.
[34] Yang T, Wang X, Liu W, Shi Y, Yang F. Double-layer anti-reflection coating containing a nanoporous anodic aluminum oxide layer for GaAs solar cells. Opt Express 2013;21(15):18207. https://doi.org/10.1364/OE.21.018207.
[35] McIntosh KR, Baker-Finch SC. OPAL 2: Rapid optical simulation of silicon solar cells. 2012 38th IEEE Photovoltaic Specialists Conference, IEEE; 2012, p. 265–71.
[36] Kulish MR, Kostylyov VP, Sachenko AV, Sokolovskyi IO, Khomenko DV, Shkrebtii AI. Luminescent converter of solar light into electrical energy review. Semiconductor Phys Quan Electron Optoelectron. 2016:229–47.
[37] Emery KA. Solar simulators and I-V measurement methods. Solar Cells 1986;18(3-4):251–60.
[38] Yahaya NA, Yamada N, Kotaki Y, Nakayama T. Characterization of light absorption in thin-film silicon with periodic nanohole arrays. Opt Express 2013;21(5):5924. https://doi.org/10.1364/OE.21.005924.
[39] Zahid Muhammad Aleem, Cho Young Hyun, Yi Junsin. Improvement in optical and electrical performance of hydrophobic andantireflective silica nanoparticles coating on PMMA for lightweightPV module. Opt Mater 2021;119. https://doi.org/10.1016/j.optmat.2021.111371. Submitted for publication.
[40] Zahid MA, Park H, Cho YH, Yi J. Plasma etched PMMA/CaF2 anti-reflection coating for light weight PV module. Opt Mater 2021;112:110813. https://doi.org/10.1016/j.optmat.2021.110813.
[41] Padilla M, Michl B, Thaidigsmann B, Warta W, Schubert MC. Short-circuit current density mapping for solar cells. Sol Energy Mater Sol Cells 2014;120:282–8.
[42] Hierrezuelo-Cardet P, Palechor-Ocampo AF, Caram J, Ventosinos F, Pérez-del-Rey D, Bolink HJ, et al. External quantum efficiency measurements used to study the stability of differently deposited perovskite solar cells. J Appl Phys 2020;127(23):235501. https://doi.org/10.1063/5.0011503.
[43] Hung M-M, Han H-V, Hong C-Y, Hong K-H, Yang T-T, Yu P, et al. Compound biomimetic structures for efficiency enhancement of Ga 0.5 In 0.5 P/GaAs/Ge triple-junction solar cells. Opt Express 2014;22:A295–300.